Geophysical Research Letters

RESEARCH LETTER
10.1029/2023GL105491

The Effects of African Easterly Wave Suppression by Wave Track on Atlantic Tropical Cyclones

Emily Bercos-Hickey[1] **and Christina M. Patricola**[1,2]

[1]Climate and Ecosystem Sciences Division, Lawrence Berkeley National Laboratory, Berkeley, CA, USA, [2]Department of Geological and Atmospheric Sciences, Iowa State University, Ames, IA, USA

Key Points:

- African easterly wave (AEW) suppression in the south track produced a larger increase in tropical cyclone (TC) activity than the north track
- Increased TC activity with AEW suppression, specifically in the south track, was associated with more favorable environmental conditions
- Suppressing south track AEWs strengthened disturbances associated with increased Atlantic rainfall that may serve as TC seeds

Supporting Information:

Supporting Information may be found in the online version of this article.

Correspondence to:

E. Bercos-Hickey,
ebercoshickey@lbl.gov

Citation:

Bercos-Hickey, E., & Patricola, C. M. (2023). The effects of African easterly wave suppression by wave track on Atlantic tropical cyclones. *Geophysical Research Letters*, *50*, e2023GL105491. https://doi.org/10.1029/2023GL105491

Received 13 JUL 2023
Accepted 3 NOV 2023

Abstract It is well established that African easterly waves (AEWs) can serve as seedling disturbances for Atlantic tropical cyclones (TCs). However, research has shown that AEWs are not necessary to maintain specifically basin-wide TC frequency. Here, we for the first time investigate the effects of AEW suppression by wave track on Atlantic TC activity. Regional model simulations were performed, where AEWs were either prescribed or suppressed from the eastern lateral boundary condition. We found that without AEWs, there was an increase in TC frequency and strength, with the most pronounced increases occurring when the waves were suppressed in the south track. These changes coincided with more favorable environmental conditions and disturbances associated with increased convective activity over the Atlantic. Our results indicate that AEWs are not a limiting factor for TCs, and that AEW suppression, specifically in the south track, can affect the large-scale environment to enhance favorability for TC genesis.

Plain Language Summary African easterly waves (AEWs) are observed in two wave tracks and can develop into tropical cyclones (TCs) over the Atlantic Ocean. However, it has been shown that the seasonal number of TCs is not affected by the absence of AEWs. In this study, we use a regional model to investigate the effects of suppressing AEWs (north track, south track, and both tracks) on TC activity. We found that without AEWs, there was an increase in the seasonal number of TCs and TC strength. The largest increases occurred when the waves were suppressed from the south wave track. These changes coincided with a more favorable environment for TCs and the emergence of AEW-like features associated with precipitation over the Atlantic Ocean. Our results indicate that AEWs are not a requirement for TCs, and that suppressing AEWs, specifically in the south wave track, can enhance conditions for TC development.

1. Introduction

African easterly waves (AEWs) are synoptic-scale disturbances that propagate westward across North Africa and over the Atlantic Ocean (Burpee, 1972; Carlson, 1969). AEWs typically have periods between 2 and 10 days and grow and propagate along the African easterly jet (AEJ) in two tracks north and south of ~15°N (Burpee, 1972; Diedhiou et al., 1998; Pytharoulis & Thorncroft, 1999; Reed et al., 1977). AEWs are of particular scientific interest because they can serve as seedling disturbances for Atlantic tropical cyclones (TCs) (Avila & Pasch, 1992; Landsea, 1993). Indeed, previous research has shown that approximately 60% of TCs and 85% of major hurricanes develop from AEWs (N. L. Frank, 1970; Landsea, 1993; Russell et al., 2017). Recent work, however, has used regional model experiments to show that suppressed AEW activity did not affect basin-wide Atlantic TC frequency (Danso et al., 2022; Patricola et al., 2018). Given that research has shown that climate change may double the economic damages of TCs by the year 2100 through increased TC intensity, precipitation, and storm surge (Knutson et al., 2020; Mendelsohn et al., 2012; Patricola & Wehner, 2018), it is imperative to better understand TC genesis and the role of AEWs.

TC genesis requires the co-occurrence of multiple factors, including weak vertical wind shear, a moist mid-troposphere, warm sea surface temperatures (SSTs), and an initial precursor or "seed" disturbance (Avila, 1991; Emanuel, 1988; W. M. Frank & Ritchie, 2001; Gray, 1968; Landsea, 1993). A seed disturbance is a convective weak vortex that is generated within the large-scale circulation (Hsieh et al., 2022), which can then evolve into a TC depending on the environmental conditions (Hoogewind et al., 2020; Hsieh et al., 2020; Tang & Camargo, 2014; Vecchi et al., 2019; Yang et al., 2021). Many previous studies have examined how convection drives AEWs and how AEWs serve as seed disturbances for TCs (Avila & Pasch, 1992; Bercos-Hickey et al., 2023; Berry & Thorncroft, 2012; Chen & Dudhia, 2001; N. L. Frank, 1970; Hopsch et al., 2007, 2009;

Landsea, 1993; Núñez Ocasio & Rios-Berrios, 2023; Russell & Aiyyer, 2020; Thorncroft & Hodges, 2001). For example, Thorncroft and Hodges (2001) found that tracked AEWs in reanalysis data were positively correlated with Atlantic TC activity between 1985 and 1998 and that TC activity was mostly associated with the south AEW track. Russell et al. (2017) used TC track data in combination with eddy kinetic energy (EKE) from reanalysis data as an estimate of AEW activity; they found a correlation between seasonal mean EKE below the south AEW track and TC genesis. Chen and Dudhia (2001) used reanalysis data to examine north and south track AEWs and found that the north track had more waves, but that the conversion rate of AEWs to TCs was twice as effective for waves from the south track.

Other studies have found that AEWs are not the driving force behind TC genesis and frequency (Caron & Jones, 2012; Danso et al., 2022; Emanuel, 2022; Hoogewind et al., 2020; Patricola et al., 2018). For example, Hoogewind et al. (2020) used TC track and reanalysis data to show that the areal extent of favorable environmental conditions does well in capturing climatological TC activity. Emanuel (2022) found that climatological TC frequency is controlled primarily by environmental conditions, such as SSTs. Patricola et al. (2018) and Danso et al. (2022) explored the relationship between AEWs and TCs by comparing ensembles of regional model simulations where AEWs in both tracks were either prescribed or suppressed through the lateral boundary conditions. Both studies found that suppressed AEW activity did not affect basin-wide Atlantic TC frequency, however neither study examined the effects of AEW suppression on the separate north and south wave tracks. The results of Patricola et al. (2018) and Danso et al. (2022) suggest that, in the absence of AEWs in both wave tracks, other mechanisms serve as the initial disturbances needed for TC genesis. Such mechanisms could include equatorial waves (including those that are westward propagating; Feng et al., 2023) or wave breaking of the Inter-Tropical Convergence Zone, where wavelike disturbances provide the seeds for Atlantic TCs (Agee, 1972; Cao et al., 2013; Feng et al., 2023; Kieu & Zhang, 2008; Lawton & Majumdar, 2023; Schreck, 2016; Thompson & Miller, 1976). TC-like phenomena have also been shown to form from self-aggregation of convection in rotating radiative-convective equilibrium simulations (Khairoutdinov & Emanuel, 2013; Wing et al., 2016; Zhou et al., 2014).

An extensive amount of research has been conducted on the relationship between AEWs and TCs using observational, reanalysis, and model data, but results are conflicting and uncertainty remains. Some studies show a strong connection between TC genesis and AEWs, specifically with waves from the south track (Chen & Dudhia, 2001; Hopsch et al., 2009; Russell et al., 2017; Thorncroft & Hodges, 2001). Other studies, however, have found that TC frequency is primarily controlled by environmental factors and that AEW suppression does not have a significant impact on TC genesis (Danso et al., 2022; Hoogewind et al., 2020; Patricola et al., 2018). In this study, our objective is to further examine the relationship between TC genesis and AEWs. We focus specifically—and for the first time—on the effects of AEW suppression by wave track and we explore possible TC genesis mechanisms in the absence of AEWs, two important knowledge gaps that were not addressed by Patricola et al. (2018) and Danso et al. (2022). It is important to note that our goal is to examine the effects of AEW suppression by wave track on Atlantic TCs; we are not suggesting that AEWs are not important TC precursors. To carry out this research, we use a suite of regional model simulations in which AEWs in the north, south, or both tracks, were either prescribed or suppressed through the lateral boundary conditions. The model and methods used in this study are presented in Section 2, while the results and conclusions are presented in Sections 3 and 4, respectively.

2. Model and Methods

The simulations were run using the Weather Research and Forecasting (WRF) model (Skamarock et al., 2008), version 3.8.1. WRF is well suited for this research as the choice of the simulation domain is flexible and WRF has been shown to realistically simulate AEWs and TCs (Bercos-Hickey & Patricola, 2021; Patricola et al., 2016). For our purposes, we are interested in the effects of suppressed AEW activity on TCs, and we therefore follow Patricola et al. (2018) and set our domain over the Atlantic Ocean and the Americas with the eastern boundary aligned with 15°W (Figure S1 in Supporting Information S1). We performed a control simulation, where AEWs enter the model domain shown in Figure S1 in Supporting Information S1 through the eastern lateral boundary. We used the objective AEW tracking algorithm from Bercos-Hickey and Patricola (2021) and found that WRF produces a similar number of AEWs as the ERA5 reanalysis and produces more AEWs in the north track than the south track as in Chen (2006) and Chen and Dudhia (2001), thus lending confidence in our control simulations. To examine the effects of AEW suppression in the north, south and both wave tracks, we conducted three

experiments, which we refer to as north filter, south filter, and both filters. The experiments had a 2–10 day band-stop filter applied to all vertical levels of the wind, temperature, geopotential, and moisture variables in the eastern lateral boundary condition between the following latitude bands: 15–30°N (north filter), 5°S–15°N (south filter), and 5°S–30°N (both filters). This filtering method suppresses the 3–5 and 6–9 day AEW signals from the individual north and south AEW tracks and both tracks (Diedhiou et al., 1998), and is consistent with Patricola et al. (2018), who examined AEW suppression in both tracks (5°S–30°N). The effects of the filtering can be seen by comparing time series of the 850 hPa meridional wind in the control and the three experiments (Figure S2 in Supporting Information S1), where the wind speed is reduced in the experiments due to the suppression of the 2–10 day signal. Additionally, vertical cross-sections of the zonal wind (Figure S3 in Supporting Information S1) demonstrate that the filtering did not render the background state unrealistic, as seen by the clear presence of the AEJ.

All simulations were run at the TC-permitting resolution of 27 km (Patricola et al., 2016), with 50 vertical layers and 3-hourly output. The simulations were performed for the years 2003, 2010, and 2011. These years were chosen because they have a similar number of TCs (16–19) and number of TCs that develop from AEWs (10–11), and average or above average accumulated cyclone energy (ACE) (Avila & Stewart, 2013; Beven & Blake, 2015; Lawrence et al., 2005), thus reducing differences between the simulations that may arise from selecting years with a large variation in TCs or developing AEWs. Ten-member ensembles of the control and experiments were generated by initializing the model with different initial conditions corresponding to May 6–15. Output up to June 1 was discarded for model spin-up, and June 1–December 1 was used for analysis. Simulated TCs were identified using an objective tracking algorithm (Walsh, 1997) and time averages were for the June 1–December 1 analysis period. Additional details are provided in Supporting Information S1.

3. Results

We begin our analysis by comparing TC frequency and strength in the control and filtering experiments. Table 1 shows the ensemble mean and standard deviation of seasonal Atlantic TC number, number of TC days, and ACE, which is the sum of the squares of the 6-hourly maximum TC wind speed throughout the life of a TC for all TCs in a season (Bell et al., 2000). For all of the TC measures, the standard deviation indicates that there is not a large variance in the response to suppressing AEW activity across the ensemble members. There were 13, 19, and 18 named TCs between June-November in 2003, 2010, and 2011, respectively (NHC, 2023). Although we would not expect WRF to exactly reproduce observations, the control does well at simulating seasonal TC frequency, with an ensemble average of 13.3, 20.2, and 14.1 TCs between June–November for 2003, 2010, and 2011, respectively.

The measures of TC activity in Table 1 are larger in the filtering experiments than in the control for all 3 years examined. The largest difference is between the control and the both filters experiment, followed by the south and north filter experiments. The differences are statistically significant, $p < 0.05$ with a two-sided t-test, for all measures in the both filters and south filter experiments of the 3 years. For the north filter experiment, the differences are statistically significant for the year 2010 and for the ACE in 2003. These results indicate that AEWs are not necessary to maintain basin-wide TC frequency, as shown by Patricola et al. (2018), and that AEW suppression can even enhance TC activity (Danso et al., 2022). Here we extend the results of Patricola et al. (2018) and Danso et al. (2022) by demonstrating that AEW suppression in the south wave track produces a larger response in TC activity than AEW suppression in the north wave track. Our finding may be somewhat surprising, but previous research has shown that TC frequency is primarily controlled by environmental conditions, with monthly mean atmospheric and oceanic states as the dominant predictors of interannual TC activity (Emanuel, 2022; Emanuel et al., 2008).

To better understand why TC frequency and strength increase in the filtering experiments, we examine the 600 hPa relative humidity and 850–200 hPa vertical wind shear, two potential indicators of environmental favorability for TC genesis (W. M. Frank & Ritchie, 2001; Hendricks et al., 2010; Kaplan et al., 2010). Figure 1 shows time- and ensemble-averaged relative humidity differences between the both, north, and south filter experiments and the control for all 3 years. Positive anomalies can be seen between 5 and 20°N in all panels of Figure 1, indicating larger mid-tropospheric relative humidity in the filtering experiments than in the control. This increase in moisture over the Atlantic in the filtering experiments is likely related to a strengthening of the AEJ (Figure S4 in Supporting Information S1), which is associated with significant easterly moisture fluxes (Cadet & Nnoli, 1987), and also coincides with a region of increased TC track density in the filtering experiments (Figure

Table 1
Measures of Simulated Atlantic Tropical Cyclone Activity in the Control and Three African Easterly Wave Filtering Experiments

		Control	Both filters	North filter	South filter
2003	Number of TCs per season	$M = 13.3$	$M = 18.8$*	$M = 14.0$	$M = 17.3$*
		SD = 1.6	SD = 3.3	SD = 2.7	SD = 2.5
			(41%)	(5%)	(30%)
	TC days per season	$M = 71.8$	$M = 99.4$*	$M = 77.5$	$M = 94.98$*
		SD = 9.6	SD = 9.6	SD = 13.9	SD = 10.7
			(38%)	(7%)	(32%)
	ACE (10^4 kt^2)	$M = 63.76$	$M = 96.88$*	$M = 77.29$*	$M = 89.65$*
		SD = 10.1	SD = 9.7	SD = 12.6	SD = 12.2
			(52%)	(21%)	(41%)
2010	Number of TCs per season	$M = 20.2$	$M = 29.6$*	$M = 24.1$*	$M = 27.3$*
		SD = 3.0	SD = 5.0	SD = 2.8	SD = 2.8
			(47%)	(19%)	(35%)
	TC days per season	$M = 101.94$	$M = 157.61$*	$M = 125.73$*	$M = 146.18$*
		SD = 10.9	SD = 25.1	SD = 14.6	SD = 12.3
			(55%)	(23%)	(43%)
	ACE (10^4 kt^2)	$M = 89.07$	$M = 147.34$*	$M = 112.43$*	$M = 133.21$*
		SD = 11.5	SD = 25.1	SD = 16.0	SD = 12.6
			(65%)	(26%)	(50%)
2011	Number of TCs per season	$M = 14.1$	$M = 20.0$*	$M = 15.2$	$M = 18.8$*
		SD = 2.8	SD = 2.6	SD = 3.7	SD = 3.7
			(42%)	(8%)	(33%)
	TC days per season	$M = 74.91$	$M = 103.59$*	$M = 78.64$	$M = 100.44$*
		SD = 15.0	SD = 15.2	SD = 17.0	SD = 15.1
			(38%)	(5%)	(34%)
	ACE (10^4 kt^2)	$M = 66.38$	$M = 93.86$*	$M = 67.42$	$M = 83.67$*
		SD = 12.7	SD = 15.5	SD = 15.4	SD = 14.2
			(41%)	(2%)	(26%)

Note. The ensemble mean and standard deviation are denoted with M and SD, respectively. The asterisks (*) indicates that the difference is statistically significant compared to the control according to a two-sided *t*-test ($p < 0.05$). Percent increases relative to the control are shown in parentheses below each standard deviation.

S5 in Supporting Information S1). The both and south filter experiments have the largest increase in relative humidity, whereas the increase in the north filter experiment is only statistically significant for 2010. This finding is consistent with Table 1, where statistical significance was primarily seen in the both and south filter experiments. The results shown in Figure 1 indicate that AEW suppression, specifically in the south track, leads to an increase in mid-tropospheric moisture, which suggests greater environmental favorability for TC development.

Next we examine the 850–200 hPa vertical wind shear. Figure 2 shows time- and ensemble-averaged vertical wind shear differences between the both, north, and south filter experiments and the control for all 3 years. Positive and negative anomalies are present throughout the Atlantic basin, primarily in the both and south filter experiments. The statistically significant anomalies between 5 and 30°N are primarily negative and occur mostly in the eastern extent of the domain, indicating regions of weaker vertical wind shear in the filtering experiments than in the control. These regions of weaker vertical wind shear also coincide with an increase in the TC track density in the filtering experiments compared to the control (Figure S5 in Supporting Information S1). The changes in vertical wind shear are likely associated with a weakening of the tropical easterly jet that is seen in the filtering experiments (Figure S4 in Supporting Information S1). Similar to Table 1 and Figure 1, the north filter experiment has the smallest effect on the vertical wind shear compared to the other two experiments. AEW suppression

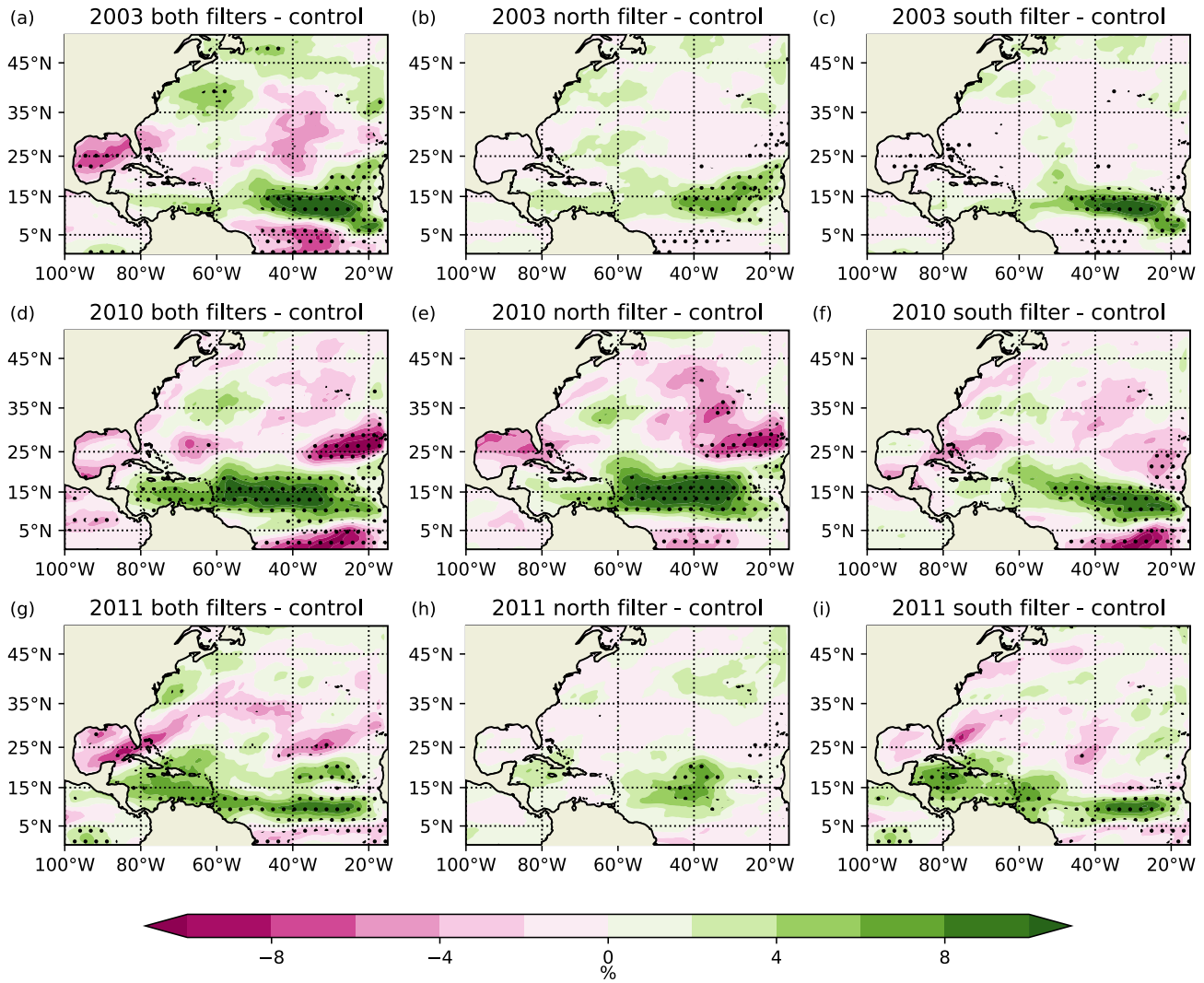

Figure 1. Time- and ensemble-averaged 600 hPa relative humidity (%) from the (a) (d) (g) both, (b) (e) (h) north, and (c) (f) (i) south filter experiments minus the control from the years (a)–(c) 2003, (d)–(f) 2010, and (g)–(i) 2011. Stippling refers to a significant difference in the relative humidity between the experiments and the control using a grid-cell specific two sample *t*-test with the *p*-values adjusted by controlling the false discovery rate at 0.05.

in the south track, however, leads to a statistically significant decrease in the vertical wind shear, and therefore more environmental favorability for TC genesis. The results presented in Figures 1 and 2 both demonstrate that AEW suppression between 5°S and 15°N is the predominate driver of increased environmental favorability for TC genesis, and thus an increase in TC frequency and strength (Table 1).

In addition to requiring a favorable environment, TCs need some type of initial disturbance for genesis (Sobel et al., 2021). Although Patricola et al. (2018) and Danso et al. (2022) found that basin-wide TC frequency was maintained despite AEW suppression, they did not explore the mechanisms responsible for genesis. Here we address this knowledge gap by examining the power spectral density (PSD) of the meridional wind at 900 and 700 hPa to identify possible precursors for TC genesis in the north and south wave tracks, respectively. We choose the PSD of the meridional wind at low levels and the jet level as this method has previously been used to identify disturbances (AEWs) north and south of the AEJ (Pytharoulis & Thorncroft, 1999). We first focus on the region of the south AEW track. Figure 3 shows the PSD of the 5°S–15°N and ensemble-averaged 700 hPa meridional wind at 20°W and 35°W for all simulations. At 20°W, all simulations show a peak between 2 and 10 days, with a notably weaker signal in the both and south filter experiments. This is not surprising as the filtering in the both and south filter experiments suppressed these disturbances. However, by 35°W there is a distinct strengthening of the 2–10 day signal in the both and south filter experiments, with the largest peaks occurring in these experiments

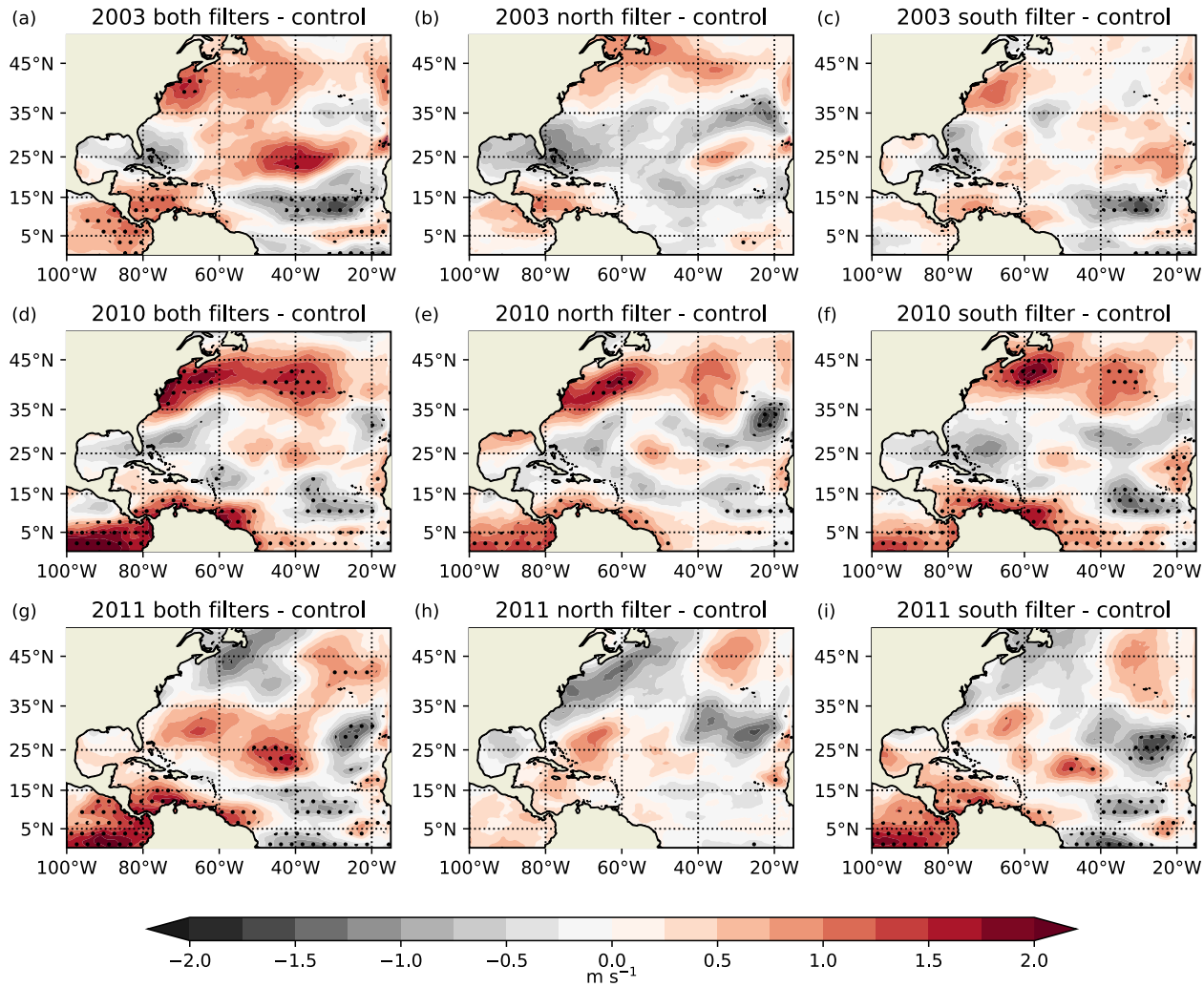

Figure 2. Time- and ensemble-averaged 850–200 hPa vertical wind shear (m s^{-1}) from the (a) (d) (g) both, (b) (e) (h) north, and (c) (f) (i) south filter experiments minus the control from the years (a)–(c) 2003, (d)–(f) 2010, and (g)–(i) 2011. Stippling refers to a significant difference in the vertical wind shear between the experiments and the control using a grid-cell specific two sample *t*-test with the *p*-values adjusted by controlling the false discovery rate at 0.05.

in 2003 and 2010. The results presented in Figure 3 suggest that disturbances similar to AEWs develop off of the coast of Africa in the experiments where AEWs were suppressed in the south track. Indeed, Hovmöller diagrams of the meridional wind indicate that these disturbances are propagating westward (Figure S6 in Supporting Information S1). In contrast, PSD of the 900 hPa meridional wind do not show a strengthening of the 2–10 day signal in the 15–30°N region when AEWs were suppressed in the north track (Figure S7 in Supporting Information S1).

To better understand the strengthening of the 2–10 day signal in the both and south filter experiments, recall that a seed disturbance is defined as a convective weak vortex that is generated within the large-scale circulation (Hsieh et al., 2022). We therefore examine convective activity in the simulations. Figure 4 shows time- and ensemble-averaged rainfall rate differences between the both, north, and south filter experiments and the control for all 3 years. Positive anomalies can be seen in Figure 4 between 5 and 15°N, with statistical significance occurring in all both and south filter experiments and the 2010 north filter experiment. These positive regions indicate a larger rainfall rate in the experiments compared to the control, and therefore more convective activity. The regions of increased convection coincide with the south AEW track and have an eastern extent of ~25–30°W, with little difference between the experiments and the control between 20°W and the eastern domain boundary. The regions of increased convection also coincide with where the 2–10 day signal strengthened in the experiments with AEW suppression in the south track (Figure 3). This suggests that when AEWs are suppressed in the south track, there is an increase in convective activity off of the coast of Africa that is associated with possible precursors to TC genesis.

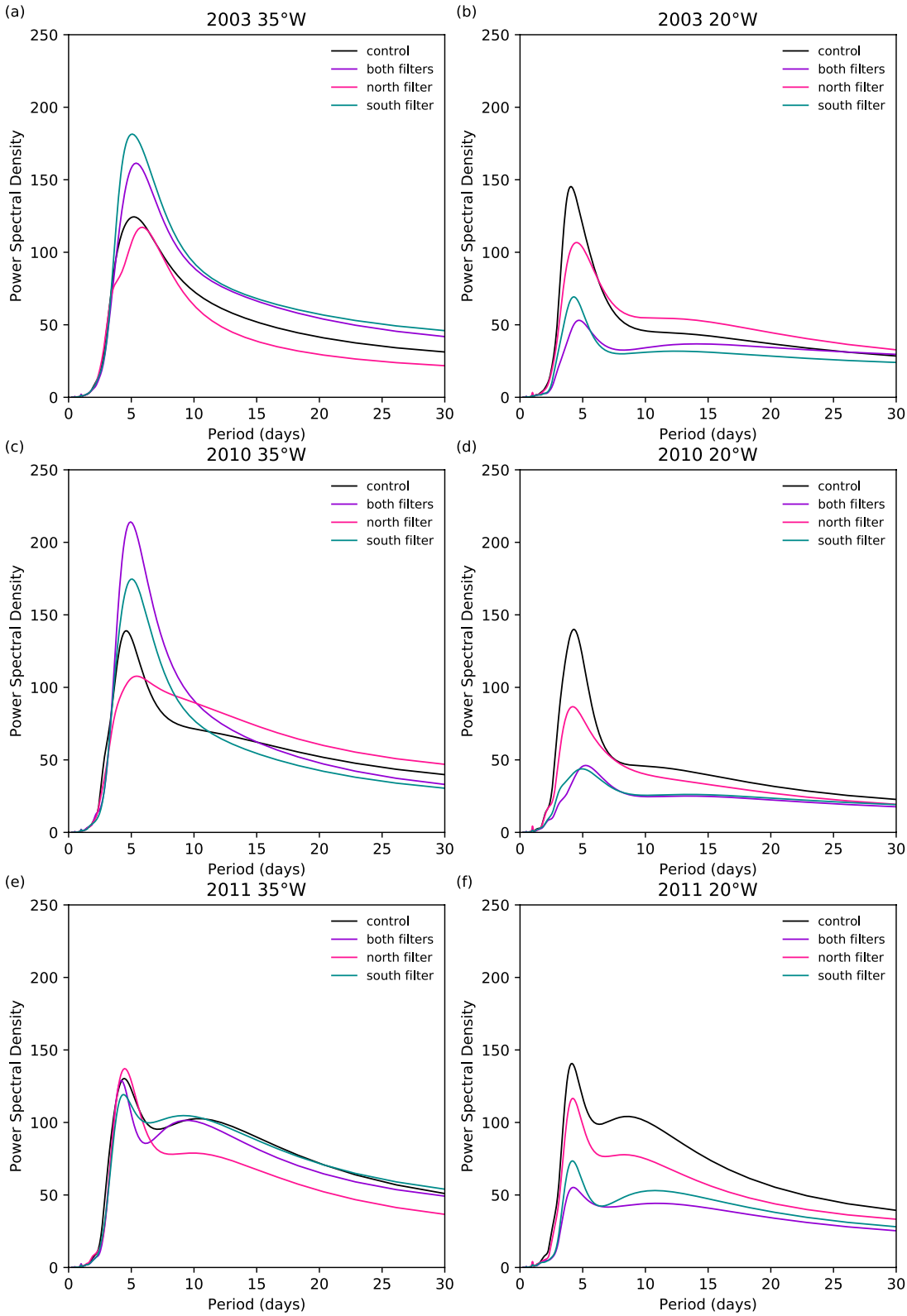

Figure 3. Power spectral density plots of the control, both, north, and south filter ensemble-averaged 700 hPa meridional wind averaged between 5°S and 15°N at (a) (c) (e) 35°W and (b) (d) (f) 20°W for the years (a) (b) 2003, (c) (d) 2010, and (e) (f) 2011.

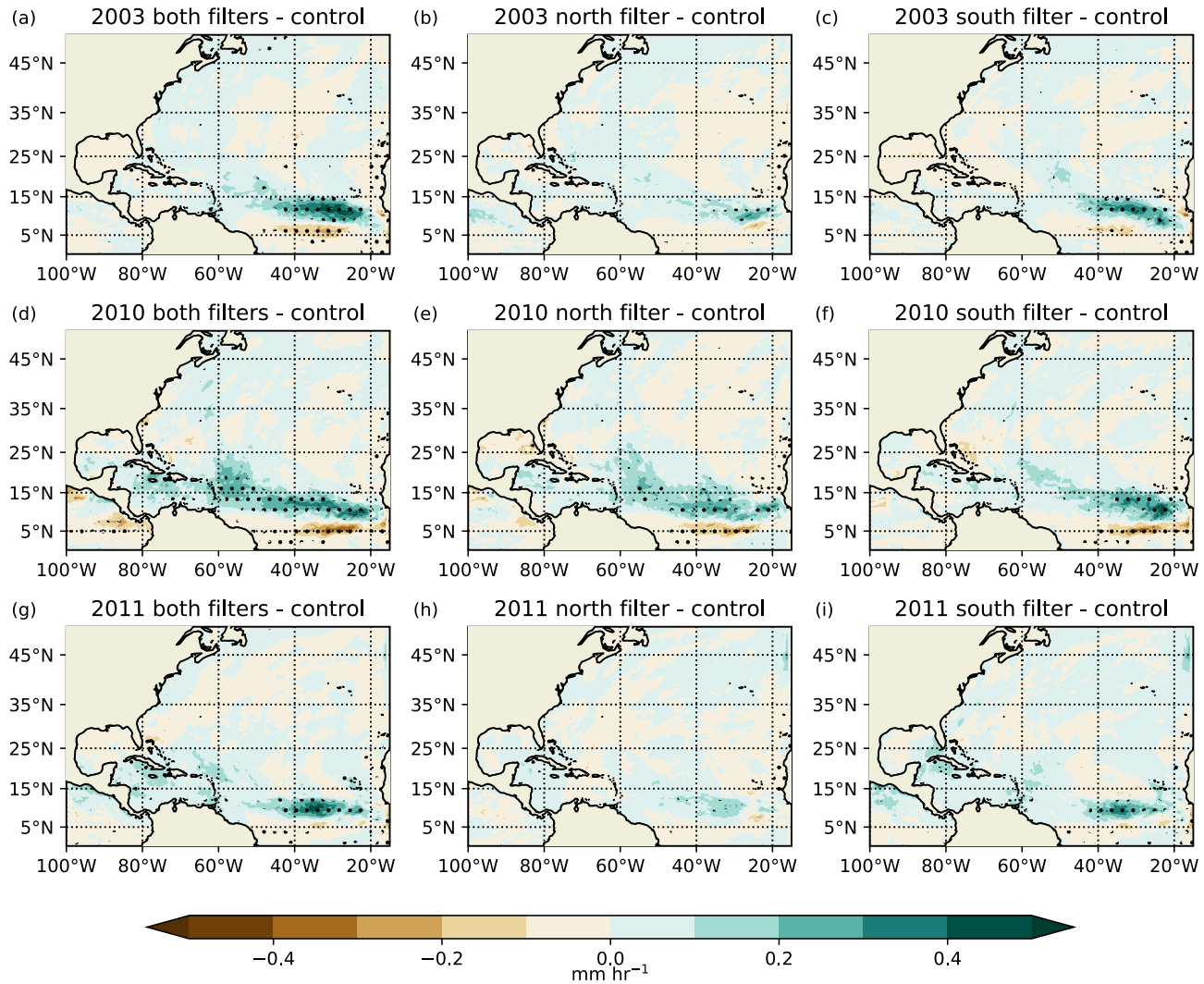

Figure 4. Time- and ensemble-averaged rainfall rate (mm hr^{-1}) from the (a) (d) (g) both, (b) (e) (h) north, and (c) (f) (i) south filter experiments minus the control from the years (a)–(c) 2003, (d)–(f) 2010, and (g)–(i) 2011. Stippling refers to a significant difference in the rainfall rate between the experiments and the control using a grid-cell specific two sample *t*-test with the *p*-values adjusted by controlling the false discovery rate at 0.05.

4. Conclusions

The mechanisms behind TC genesis have been the subject of numerous studies, but knowledge gaps remain. Previous research has shown that AEWs can serve as seedling disturbances for TCs forming in the Atlantic Ocean (Avila & Pasch, 1992; Chen & Dudhia, 2001; Landsea, 1993; Russell et al., 2017). However, other studies have shown that favorable environmental conditions are primarily responsible for TC genesis (Emanuel, 2022; Emanuel et al., 2008; Saunders et al., 2017), and that AEW suppression did not affect basin-wide TC frequency (Danso et al., 2022; Patricola et al., 2018). In this study, we examine the relationship between TC genesis and AEWs by specifically looking at how TC frequency is affected by the suppression of AEWs in both wave tracks and the north and south tracks individually. To conduct this research, we used a suite of regional model simulations in which AEWs were either prescribed (control) or suppressed through the lateral boundary conditions. We found that AEW suppression led to an increase in TC frequency and strength as well as more favorable environmental conditions for TC genesis. These findings were primarily driven by AEW suppression in the south track, and were associated with the emergence of disturbances over the Atlantic that coincide with increased convective activity.

Seasonal TC frequency, number of TC days, and ACE were all larger in the AEW suppression experiments than in the control, with the largest and statistically significant differences occurring in the experiments where the

south track waves were suppressed. These results suggest that in the absence of AEWs, other mechanisms are driving TC genesis, such as the large-scale environment (Emanuel, 2022; Emanuel et al., 2008). We found that there was an increase in mid-tropospheric relative humidity and a decrease in vertical wind shear in the AEW suppression experiments compared to the control. This indicates that suppressing AEWs leads to more favorable environmental conditions for TC genesis, in agreement with Danso et al. (2022). In this study, however, the increase in environmental favorability was more pronounced and statistically significant in the experiments with AEW suppression in the south track.

Despite AEW suppression resulting in more favorable environmental conditions, TC genesis requires some type of initial disturbance. By examining the PSD of the meridional wind, we found a strengthening of the 2–10 day signal between 5°S and 15°N and near 35°W in the experiments with AEW suppression in the south track. This suggests that disturbances similar to AEWs develop off of the coast of Africa in the region of the south track in the absence of AEWs. It is possible that these disturbances are driven by some of the same dynamical mechanisms as AEWs over the Atlantic Ocean, but, due to the filtering, we know that the disturbances are not AEWs. A statistically significant increase in rainfall also occurs in the same region in the experiments where AEWs were suppressed in the south track when compared to the control. Given that convective vortices can serve as TC seeds (Hsieh et al., 2022), it is likely that the aforementioned increase in precipitation results in the emergence of disturbances that could lead to TC genesis.

Our results demonstrate that not only are AEWs not necessary to maintain basin-wide TC frequency, but that the absence of AEWs can lead to an increase in TC frequency and strength. It is important to note, however, that the results presented here in no way suggest that AEWs are not important precursors to TCs. Our findings are also limited by the sample size of our simulations as well as the model resolution. Additional data would add to the robustness of our results, specifically by examining years with varying TC and AEW activity. Running multiple seasons at a finer resolution would also allow the model to simulate major hurricanes, which are more likely to form from AEWs (N. L. Frank, 1970; Landsea, 1993; Russell et al., 2017). We have, however, demonstrated that in the absence of AEWs, there are other mechanisms that lead to TC genesis. Future work is needed to better understand how the large-scale environment, AEWs, and other disturbances interact to drive TC development in the Atlantic.

Data Availability Statement

The climate model output used in this study is available via Bercos-Hickey and Patricola (2023). The TC tracking code used for analysis is available on GitHub via Bercos-Hickey (2023).

Acknowledgments
This material is based upon work supported by the U.S. Department of Energy, Office of Science, Office of Biological and Environmental Research, Climate and Environmental Sciences Division, Regional & Global Model Analysis Program, under Award Number DE-AC02-05CH11231. C.M.P. acknowledges support from the U.S. Department of Energy, Office of Science, Office of Biological and Environmental Research, Earth and Environmental Systems Modeling (EESM) Program, Early Career Research Program Award Number DE-SC0021109. This research used resources of the National Energy Research Scientific Computing Center (NERSC), a U.S. Department of Energy Office of Science User Facility operated under Contract No. DE-AC02-05CH11231.

References

Agee, E. M. (1972). Note on ITCZ wave disturbances and formation of tropical storm Anna. *Monthly Weather Review*, *100*(10), 733–737. https://doi.org/10.1175/1520-0493(1972)100<0733:NOIWDA>2.3.CO;2

Avila, L. A. (1991). Atlantic tropical systems of 1990. *Monthly Weather Review*, *119*(8), 2027–2033. https://doi.org/10.1175/1520-0493(1991)119<2027:ATSO>2.0.CO;2

Avila, L. A., & Pasch, R. J. (1992). Atlantic tropical systems of 1991. *Monthly Weather Review*, *120*(11), 2688–2696. https://doi.org/10.1175/1520-0493(1992)120<2688:ATSO>2.0.CO;2

Avila, L. A., & Stewart, S. R. (2013). Atlantic hurricane season of 2011. *Monthly Weather Review*, *141*(8), 2577–2596. https://doi.org/10.1175/MWR-D-12-00230.1

Bell, G. D., Halpert, M. S., Schnell, R. C., Higgins, R. W., Lawrimore, J., Kousky, V. E., et al. (2000). Climate assessment for 1999. *Bulletin of the American Meteorological Society*, *81*(6), S1–S50. https://doi.org/10.1175/1520-0477(2000)81[s1:CAF]2.0.CO;2

Bercos-Hickey, E. (2023). Tropical cyclone tracker [Software]. GitHub. https://github.com/mehtut/

Bercos-Hickey, E., & Patricola, C. M. (2021). Anthropogenic influences on the African easterly jet–African easterly wave system. *Climate Dynamics*, *57*(9–10), 2779–2792. https://doi.org/10.1007/s00382-021-05838-1

Bercos-Hickey, E., & Patricola, C. M. (2023). The effects of African easterly wave suppression by wave track on Atlantic tropical cyclones [Dataset]. https://portal.nersc.gov/archive/home/projects/cascade/www/AEW_Suppression

Bercos-Hickey, E., Patricola, C. M., Loring, B., & Collins, W. D. (2023). The relationship between African easterly waves and tropical cyclones in historical and future climates in the HighResMIP-PRIMAVERA simulations. *Journal of Geophysical Research: Atmospheres*, *128*(7), e2022JD037471. https://doi.org/10.1029/2022JD037471

Berry, G. J., & Thorncroft, C. D. (2012). African easterly wave dynamics in a mesoscale numerical model: The upscale role of convection. *Journal of the Atmospheric Sciences*, *69*(4), 1267–1283. https://doi.org/10.1175/JAS-D-11-099.1

Beven, J. L., II, & Blake, E. S. (2015). Atlantic hurricane season of 2010. *Monthly Weather Review*, *143*(9), 3329–3353. https://doi.org/10.1175/MWR-D-11-00264.1

Burpee, R. W. (1972). The origin and structure of easterly waves in the lower troposphere of north Africa. *Journal of the Atmospheric Sciences*, *29*(1), 77–90. https://doi.org/10.1175/1520-0469(1972)029<0077:TOASOE>2.0.CO;2

Cadet, D. L., & Nnoli, N. O. (1987). Water vapour transport over Africa and the Atlantic Ocean during summer 1979. *Quarterly Journal of the Royal Meteorological Society*, *113*(476), 581–602. https://doi.org/10.1002/qj.49711347609

Cao, X., Chen, G., & Chen, W. (2013). Tropical cyclogenesis induced by ITCZ breakdown in association with synoptic wave train over the western North Pacific. *Atmospheric Science Letters*, *14*(4), 294–300. https://doi.org/10.1002/asl2.452

Carlson, T. N. (1969). Synoptic histories of three African disturbances that developed into Atlantic hurricanes. *Monthly Weather Review*, *97*(3), 256–276. https://doi.org/10.1175/1520-0493(1969)097<0256:SHOTAD>2.3.CO;2

Caron, L.-P., & Jones, C. G. (2012). Understanding and simulating the link between African easterly waves and Atlantic tropical cyclones using a regional climate model: The role of domain size and lateral boundary conditions. *Climate Dynamics*, *39*(1–2), 113–135. https://doi.org/10.1007/s00382-011-1160-8

Chen, T.-C. (2006). Characteristics of African easterly waves depicted by ECMWF reanalyses for 1991–2000. *Monthly Weather Review*, *134*(12), 3539–3566. https://doi.org/10.1175/MWR3259.1

Chen, T.-C., Wang, S.-Y., & Clark, A. J. (2008). North Atlantic hurricanes contributed by African easterly waves north and south of the African easterly jet. *Journal of Climate*, *21*(24), 6767–6776. https://doi.org/10.1175/2008JCLI2523.1

Danso, D. K., Patricola, C. M., & Bercos-Hickey, E. (2022). Influence of African easterly wave suppression on Atlantic tropical cyclone activity in a convection-permitting model. *Geophysical Research Letters*, *49*(22), e2022GL100590. https://doi.org/10.1029/2022GL100590

Diedhiou, A., Janicot, S., Viltard, A., & de Felice, P. (1998). Evidence of two regimes of easterly waves over West Africa and the tropical Atlantic. *Geophysical Research Letters*, *25*(15), 2805–2808. https://doi.org/10.1029/98GL02152

Emanuel, K. (2022). Tropical cyclone seeds, transition probabilities, and Genesis. *Journal of Climate*, *35*(11), 3557–3566. https://doi.org/10.1175/JCLI-D-21-0922.1

Emanuel, K., Sundararajan, R., & Williams, J. (2008). Hurricanes and global warming: Results from downscaling IPCC AR4 simulations. *Bulletin of the American Meteorological Society*, *89*(3), 347–368. https://doi.org/10.1175/BAMS-89-3-347

Emanuel, K. A. (1988). The maximum intensity of hurricanes. *Journal of the Atmospheric Sciences*, *45*(7), 1143–1155. https://doi.org/10.1175/1520-0469(1988)045<1143:TMIOH>2.0.CO;2

Feng, X., Yang, G.-Y., Hodges, K. I., & Methven, J. (2023). Equatorial waves as useful precursors to tropical cyclone occurrence and intensification. *Nature Communications*, *14*(1), 511. https://doi.org/10.1038/s41467-023-36055-5

Frank, N. L. (1970). Atlantic tropical systems of 1969. *Monthly Weather Review*, *98*(4), 307–314. https://doi.org/10.1175/1520-0493(1970)098<0307:ATSO>2.3.CO;2

Frank, W. M., & Ritchie, E. A. (2001). Effects of vertical wind shear on the intensity and structure of numerically simulated hurricanes. *Monthly Weather Review*, *129*(9), 2249–2269. https://doi.org/10.1175/1520-0493(2001)129<2249:EOVWSO>2.0.CO;2

Gray, W. M. (1968). Global view of the origin of tropical disturbances and storms. *Monthly Weather Review*, *96*(10), 669–700. https://doi.org/10.1175/1520-0493(1968)096<0669:GVOTOO>2.0.CO;2

Hendricks, E. A., Peng, M. S., Fu, B., & Li, T. (2010). Quantifying environmental control on tropical cyclone intensity change. *Monthly Weather Review*, *138*(8), 3243–3271. https://doi.org/10.1175/2010MWR3185.1

Hoogewind, K. A., Chavas, D. R., Schenkel, B. A., & O'Neill, M. E. (2020). Exploring controls on tropical cyclone count through the geography of environmental favorability. *Journal of Climate*, *33*(5), 1725–1745. https://doi.org/10.1175/JCLI-D-18-0862.1

Hopsch, S. B., Thorncroft, C. D., Hodges, K., & Aiyyer, A. (2007). West African storm tracks and their relationship to Atlantic tropical cyclones. *Journal of Climate*, *20*(11), 2468–2483. https://doi.org/10.1175/JCLI4139.1

Hopsch, S. B., Thorncroft, C. D., & Tyle, K. R. (2009). Analysis of African easterly wave structures and their role in influencing tropical cyclogenesis. *Monthly Weather Review*, *138*(4), 1399–1419. https://doi.org/10.1175/2009MWR2760.1

Hsieh, T.-L., Vecchi, G. A., Yang, W., Held, I. M., & Garner, S. T. (2020). Large-scale control on the frequency of tropical cyclones and seeds: A consistent relationship across a hierarchy of global atmospheric models. *Climate Dynamics*, *55*(11–12), 3177–3196. https://doi.org/10.1007/s00382-020-05446-5

Hsieh, T.-L., Yang, W., Vecchi, G. A., & Zhao, M. (2022). Model spread in the tropical cyclone frequency and seed propensity index across global warming and ENSO-like perturbations. *Geophysical Research Letters*, *49*(7), e2021GL097157. https://doi.org/10.1029/2021gl097157

Kaplan, J., DeMaria, M., & Knaff, J. A. (2010). A revised tropical cyclone rapid intensification index for the Atlantic and eastern north Pacific basins. *Weather and Forecasting*, *25*(1), 220–241. https://doi.org/10.1175/2009WAF2222280.1

Khairoutdinov, M., & Emanuel, K. (2013). Rotating radiative-convective equilibrium simulated by a cloud-resolving model. *Journal of Advances in Modeling Earth Systems*, *5*(4), 816–825. https://doi.org/10.1002/2013MS000253

Kieu, C. Q., & Zhang, D.-L. (2008). Genesis of tropical storm Eugene (2005) from merging vortices associated with ITCZ breakdowns. Part I: Observational and modeling analyses. *Journal of the Atmospheric Sciences*, *65*(11), 3419–3439. https://doi.org/10.1175/2008JAS2605.1

Knutson, T., Camargo, S. J., Chan, J. C. L., Emanuel, K., Ho, C. H., Kossin, J., et al. (2020). Tropical cyclones and climate change assessment: Part II: Projected response to anthropogenic warming. *Bulletin of the American Meteorological Society*, *101*(3), E303–E322. https://doi.org/10.1175/BAMS-D-18-0194.1

Landsea, C. W. (1993). A climatology of intense (or major) Atlantic hurricanes. *Monthly Weather Review*, *121*(6), 1703–1713. https://doi.org/10.1175/1520-0493(1993)121<1703:ACOIMA>2.0.CO;2

Lawrence, M. B., Avila, L. A., Beven, J. L., Franklin, J. L., Pasch, R. J., & Stewart, S. R. (2005). Atlantic hurricane season of 2003. *Monthly Weather Review*, *133*(6), 1744–1773. https://doi.org/10.1175/MWR2940.1

Lawton, Q. A., & Majumdar, S. J. (2023). Convectively coupled Kelvin waves and tropical cyclogenesis: Connections through convection and moisture. *Monthly Weather Review*, *151*(7), 1647–1666. https://doi.org/10.1175/MWR-D-23-0005.1

Mendelsohn, R., Emanuel, K., Chonabayashi, S., & Bakkensen, L. (2012). The impact of climate change on global tropical cyclone damage. *Nature Climate Change*, *2*(3), 205–209. https://doi.org/10.1038/nclimate1357

NHC. (2023). National hurricane center's tropical cyclone reports.

Núñez Ocasio, K. M., & Rios-Berrios, R. (2023). African easterly wave evolution and tropical cyclogenesis in a pre-helene (2006) hindcast using the model for prediction across scales-atmosphere (MPAS-A). *Journal of Advances in Modeling Earth Systems*, *15*(2), e2022MS003181. https://doi.org/10.1029/2022MS003181

Patricola, C. M., Chang, P., & Saravanan, R. (2016). Degree of simulated suppression of Atlantic tropical cyclones modulated by flavour of El Niño. *Nature Geoscience*, *9*(2), 155–160. https://doi.org/10.1038/ngeo2624

Patricola, C. M., Saravanan, R., & Chang, P. (2018). The response of Atlantic tropical cyclones to suppression of African easterly waves. *Geophysical Research Letters*, *45*(1), 471–479. https://doi.org/10.1002/2017GL076081

Patricola, C. M., & Wehner, M. F. (2018). Anthropogenic influences on major tropical cyclone events. *Nature*, *563*(7731), 339–346. https://doi.org/10.1038/s41586-018-0673-2

Pytharoulis, I., & Thorncroft, C. D. (1999). The low-level structure of African easterly waves in 1995. *Monthly Weather Review*, *127*(10), 2266–2280. https://doi.org/10.1175/1520-0493(1999)127<2266:TLLSOA>2.0.CO;2

Reed, R. J., Norquist, D. C., & Recker, E. E. (1977). The structure and properties of African wave disturbances as observed during phase III of GATE. *Monthly Weather Review*, *105*(3), 317–333. https://doi.org/10.1175/1520-0493(1977)105<0317:TSAPOA>2.0.CO;2

Russell, J. O., Aiyyer, A., White, J. D., & Hannah, W. (2017). Revisiting the connection between African easterly waves and Atlantic tropical cyclogenesis. *Geophysical Research Letters*, *44*(1), 587–595. https://doi.org/10.1002/2016GL071236

Russell, J. O. H., & Aiyyer, A. (2020). The potential vorticity structure and dynamics of African easterly waves. *Journal of the Atmospheric Sciences*, *77*(3), 871–890. https://doi.org/10.1175/JAS-D-19-0019.1

Saunders, M. A., Klotzbach, P. J., & Lea, A. S. R. (2017). Replicating annual North Atlantic hurricane activity 1878–2012 from environmental variables. *Journal of Geophysical Research: Atmospheres*, *122*(12), 6284–6297. https://doi.org/10.1002/2017JD026492

Schreck, C. J. (2016). Convectively coupled Kelvin waves and tropical cyclogenesis in a semi-Lagrangian framework. *Monthly Weather Review*, *144*(11), 4131–4139. https://doi.org/10.1175/MWR-D-16-0237.1

Skamarock, W. C., Klemp, J. B., Dudhia, J., Gill, D. O., Barker, D., Duda, M. G., et al. (2008). A description of the advanced research WRF Version 3 NCAR Tech Note NCAR/TN-475+STR. https://doi.org/10.5065/D68S4MVH

Sobel, A. H., Wing, A. A., Camargo, S. J., Patricola, C. M., Vecchi, G. A., Lee, C., & Tippett, M. K. (2021). Tropical cyclone frequency. *Earth's Future*, *9*(12), e2021EF002275. https://doi.org/10.1029/2021EF002275

Tang, B., & Camargo, S. J. (2014). Environmental control of tropical cyclones in CMIP5: A ventilation perspective. *Journal of Advances in Modeling Earth Systems*, *6*(1), 115–128. https://doi.org/10.1002/2013MS000294

Thompson, O. E., & Miller, J. (1976). Hurricane carmen: August–September 1974—Development of a wave in the ITCZ. *Monthly Weather Review*, *104*(5), 1194–1199. https://doi.org/10.1175/1520-0493(1976)104<0656:hcaoaw>2.0.co;2

Thorncroft, C. D., & Hodges, K. (2001). African easterly wave variability and its relationship to Atlantic tropical cyclone activity. *Journal of Climate*, *14*(6), 1166–1179. https://doi.org/10.1175/1520-0442(2001)014<1166:AEWVAI>2.0.CO;2

Vecchi, G. A., Delworth, T. L., Murakami, H., Underwood, S. D., Wittenberg, A. T., Zeng, F., et al. (2019). Tropical cyclone sensitivities to CO_2 doubling: Roles of atmospheric resolution, synoptic variability and background climate changes. *Climate Dynamics*, *53*(9–10), 5999–6033. https://doi.org/10.1007/s00382-019-04913-y

Walsh, K. (1997). Objective detection of tropical cyclones in high-resolution analyses. *Monthly Weather Review*, *125*(8), 1767–1779. https://doi.org/10.1175/1520-0493(1997)125<1767:ODOTCI>2.0.CO;2

Wing, A. A., Camargo, S. J., & Sobel, A. H. (2016). Role of radiative–convective feedbacks in spontaneous tropical cyclogenesis in idealized numerical simulations. *Journal of the Atmospheric Sciences*, *73*(7), 2633–2642. https://doi.org/10.1175/JAS-D-15-0380.1

Yang, W., Hsieh, T.-L., & Vecchi, G. A. (2021). Hurricane annual cycle controlled by both seeds and Genesis probability. *Proceedings of the National Academy of Sciences of the United States of America*, *118*(41), e2108397118. https://doi.org/10.1073/pnas.2108397118

Zhou, W., Held, I. M., & Garner, S. T. (2014). Parameter study of tropical cyclones in rotating radiative–convective equilibrium with column physics and resolution of a 25-km GCM. *Journal of the Atmospheric Sciences*, *71*(3), 1058–1069. https://doi.org/10.1175/JAS-D-13-0190.1

References From the Supporting Information

Chen, F., & Dudhia, J. (2001). Coupling an advanced land surface–hydrology model with the Penn state–NCAR MM5 modeling system. Part I: Model implementation and sensitivity. *Monthly Weather Review*, *129*(4), 569–585. https://doi.org/10.1175/1520-0493(2001)129<0569:CAALSH>2.0.CO;2

Dudhia, J. (1989). Numerical study of convection observed during the winter monsoon experiment using a mesoscale two-dimensional model. *Journal of the Atmospheric Sciences*, *46*(20), 3077–3107. https://doi.org/10.1175/1520-0469(1989)046<3077:NSOCOD>2.0.CO;2

Fu, D., Chang, P., Patricola, C. M., & Saravanan, R. (2019). High-resolution tropical channel model simulations of tropical cyclone climatology and intraseasonal-to-interannual variability. *Journal of Climate*, *32*(22), 7871–7895. https://doi.org/10.1175/JCLI-D-19-0130.1

Han, J., & Pan, H.-L. (2011). Revision of convection and vertical diffusion schemes in the NCEP global forecast system. *Weather and Forecasting*, *26*(4), 520–533. https://doi.org/10.1175/WAF-D-10-05038.1

Hersbach, H., Bell, B., Berrisford, P., Hirahara, S., Horányi, A., Muñoz-Sabater, J., et al. (2020). The ERA5 global reanalysis. *Quarterly Journal of the Royal Meteorological Society*, *146*(730), 1999–2049. https://doi.org/10.1002/qj.3803

Hong, S.-Y., Noh, Y., & Dudhia, J. (2006). A new vertical diffusion package with an explicit treatment of entrainment processes. *Monthly Weather Review*, *134*(9), 2318–2341. https://doi.org/10.1175/MWR3199.1

Lin, Y.-L., Farley, R. D., & Orville, H. D. (1983). Bulk parameterization of the snow field in a cloud model. *Journal of Climate and Applied Meteorology*, *22*(6), 1065–1092. https://doi.org/10.1175/1520-0450(1983)022<1065:BPOTSF>2.0.CO;2

Mlawer, E. J., Taubman, S. J., Brown, P. D., Iacono, M. J., & Clough, S. A. (1997). Radiative transfer for inhomogeneous atmospheres: RRTM, a validated correlated-k model for the longwave. *Journal of Geophysical Research*, *102*(D14), 16663–16682. https://doi.org/10.1029/97JD00237

Monin, A. S., & Obukhov, A. M. (1954). Basic laws of turbulent mixing in the surface layer of the atmosphere. *Contrib. Geophys. Inst. Acad. Sci. USSR*, *151*, e187.